Effects of reversible and irreversible ferroelectric switchings on the piezoelectric large-signal response of lead zirconate titanate thin films

P. Gerber, C. Kügeler, U. Böttger, and R. Waser

Citation: Journal of Applied Physics **98**, 124101 (2005);
View online: https://doi.org/10.1063/1.2146055
View Table of Contents: http://aip.scitation.org/toc/jap/98/12
Published by the American Institute of Physics

Effects of reversible and irreversible ferroelectric switchings on the piezoelectric large-signal response of lead zirconate titanate thin films

P. Gerber,[a] C. Kügeler, U. Böttger, and R. Waser
Institute of Materials in Electrical Engineering and Information Technology 2, (IWE2), Aachen University, D-52074 Aachen, Germany

(Received 29 July 2005; accepted 3 November 2005; published online 20 December 2005)

The effects of reversible and irreversible switching processes on the electromechanical large-signal strain S of tetragonal $Pb(Zr_x,Ti_{1-x})O_3$ thin films are investigated and discussed. Starting from electric small- and large-signal measurements, the percentage of switched unit cells ce_{sw} is calculated. The result is then used in combination with the measured electromechanical field-induced small-signal response to calculate the field-induced large-signal strain S. Enhanced models for this calculation are developed improving a known model. Differences between the calculated and measured large-signal strains are discussed in respect to parameter influences and irreversible contributions. In addition, detailed insight on the switching processes in respect to the electromechanical properties is given. © *2005 American Institute of Physics*.
[DOI: 10.1063/1.2146055]

I. INTRODUCTION

Ferroelectric $Pb(Zr_x,Ti_{1-x})O_3$ ($PZT(x/1-x)$) ceramics exhibit superior ferroelectric, piezoelectric, and pyroelectric properties. Therefore, these materials are used in a wide range of applications such as actuators, force sensors, optical infrared sensors, and ferroelectric memories. In order to use these ceramics to their full potential, thorough research of their properties is needed.[1–3]

One object of the research done up to now was to distinguish the intrinsic and extrinsic contributions to the electric and electromechanical responses of the material.[4–10] One approach is to measure the piezoelectric small-signal response of the material caused by intrinsic (reversible) effects and compare the integrated measurement results with the measured large-signal response caused by reversible and irreversible (extrinsic) effects. Hence, the intrinsic and extrinsic contributions can be separated.[10]

As shown by Taylor and Damjanovic,[8] the piezoelectric large-signal strain of (111)-oriented, tetragonal PZT thin films is caused mainly by intrinsic effects. In this material, the movement of domain walls has nearly no effect on the piezoelectric-induced strain due to the possible orientations of the polarization vectors inside the film.[8,9] Hence, piezoelectric strain is mainly caused by a shift of the Ti/Zr ions out of their stable state in combination with a geometric distortion of the unit cells. This can be considered as a shift of the Ti/Zr sublattice against the Pb/O sublattice. Therefore, these sublattice shifts can be investigated with only minor contribution caused by domain-wall movement.

Using this fact, it is possible to calculate the field-induced electromechanical large-signal strain S directly from the measurement of the field-induced electromechanical small-signal response, if the applied model considers also indirect extrinsic contributions, as they were found in Ref. 11.

A model was used by Bolten *et al.*[12] This model introduced two discontinuous jumps of the strain at the respective coercive voltages. It is, however, limited to very "hard" PZT materials with nearly absent backswitching during the transition from saturation to the remanent state. It also fails to explain the fact why the measured strain curve is "open" in saturation while the curve of the piezoelectric coefficient $d_{33,\mathrm{eff}}$ is "closed." To explain these terms, one should consider that during measurements in PZT thin films, the last part of the $d_{33,\mathrm{eff}}$ curve going to saturation shows the same $d_{33,\mathrm{eff}}$ values as the part going back from saturation to the remanent state.[11] In some cases, even higher $d_{33,\mathrm{eff}}$ values were seen for increasing bias fields than the values measured going back to remanence (crossing paths in saturations).[13] Finding an explanation for this behavior, which is contradictory to the one seen in electric measurements, is thus one of the goals of our work.

It is necessary to understand the effects of unit-cell switching or domain-wall motions on the electromechanical properties to find such an explanation. Hence, it is mandatory to improve the calculation model for the large-signal strain by introducing the indirect extrinsic influences found in Ref. 11.

II. SAMPLE PREPARATION AND PROPERTY MEASUREMENT

The PZT (45/55) thin films are prepared using chemical solution deposition (CSD) on double-side polished $Pt(111)/TiO_2/SiO_2/Si$ substrates (1 in. $\times$ 1 in. $\times$ 0.5 mm). After spin coating and pyrolysis of three coatings, the films are annealed in oxygen using rapid thermal annealing at 700° for 5 min. This results in a film thickness of 130 nm. Pt top electrodes are sputter deposited with electrode areas ranging from 0.1 to 1 mm^2. The backside is finally an evaporation deposited with Au to achieve a better reflectivity during interferometric measurements.

[a]Electronic mail: gerber@iwe.rwth-aachen.de

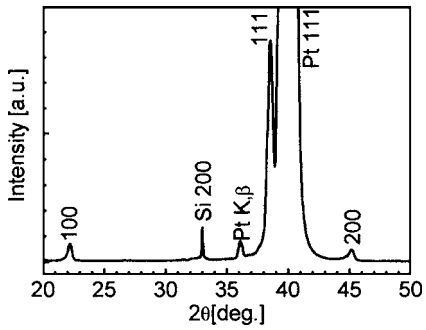

FIG. 1. X-ray-diffraction scan of 130 nm PZT (45/55) measured after complete sample preparation.

Film orientation was determined by standard θ-2θ x-ray diffraction (XRD) and sample thickness is measured by a Dektak profilometer. The piezoelectric weak-signal coefficient d_{33}, large-signal strain S, and electrostriction coefficient M_{33} are measured using a double-beam laser interferometer with a minimum resolution of 0.2 pm. For coefficient determination, the fast measurement method proposed in Ref. 14 is used. For this work, only electrodes with an area of 1 mm^2 were used in order to minimize pad size influences.[13]

III. RESULTS

Figure 1 depicts the XRD measurements done to determine the orientation of the fabricated sample. The measured PZT (45/55) samples are highly (111) oriented and show an a/c ratio >1.021 (calculated peak positions). No secondary orientation peaks are found, indicating that no rhombohedral phase is present in the samples. Also, the absence of a (001) peak and the low intensity of the (100) peak lead to the conclusion that most cells involved in switching are (111) oriented. All measurements investigate PZT (45/55), since its piezoelectric response is larger than that of, e.g., PZT (40/60) or PZT (30/70) and its composition is far away enough from the morphotropic phase boundary to exhibit only tetragonal switching.[15,16]

The electric small-signal response shown in Fig. 2 was measured in order to investigate the reversible processes in the sample. As shown in Ref. 12, integration of this result by

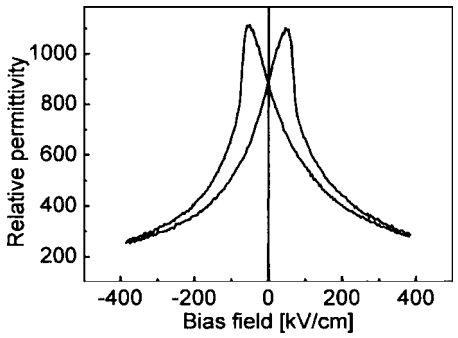

FIG. 2. Electric small-signal response measured on 130 nm PZT (45/55) ($f_{bias}=1$ Hz, $f_{ac}=8$ kHz, and $V_{ac}=100$ mV).

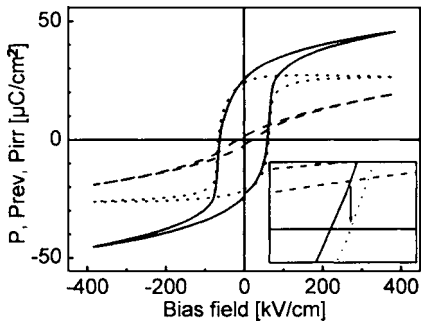

FIG. 3. Measured large-signal polarization P (line, $f_{hyst}=100$ Hz), calculated reversible polarization P_{rev} (dashes), and calculated irreversible polarization P_{irr} (dots) of 130 nm PZT (45/55).

$$P_{rev} = \frac{1}{A}\int C(V)dV \tag{1}$$

can be used to calculate the reversible contribution to the electric large-signal polarization. Figure 3 depicts both the measured large-signal polarization P and the calculated reversible contribution P_{rev}. After the curves have been symmetrized, the irreversible contribution to the polarization P_{irr} can be gained by the subtraction of both curves:

$$P = P_{rev} + P_{irr} \Rightarrow P_{irr} = P - P_{rev}. \tag{2}$$

The result of this calculation is also shown in Fig. 3.

The irreversible contribution is solely composed of extrinsic switching effects, since intrinsic lattice shifts are reversible and therefore accounted for in the reversible response measured. Hence, this result can be used to gain a quantitative insight on the configuration of the domains or unit cells, e.g., how many unit cells are switched in the positive Z direction. Of course, since most of the unit cells contributing to switching are (111) oriented, their vector of spontaneous polarization does not point directly in the Z direction but can be projected along the Z axis. Nonetheless, we can define and calculate ce_{sw}, which is the percentage of cells switched "upwards," meaning their projected spontaneous polarization vector points into the positive Z direction.

Before using ce_{sw} in further calculations, one should note the fact depicted in the inset of Fig. 3. Here, the proximity of the positive coercive voltage is zoomed in for a detailed analysis. As can be seen, the curve of the large-signal polarization P and the curve of the irreversible contribution P_{irr} cross the zero value at different bias field strengths. Since the P_{irr} is a figure for the unit cells switched, its zero crossing is the point when exactly half of the contributing unit cells are switched upwards and the other half are switched downwards. The electric field applied at this particular sample state is not the coercive field, since the coercive field is defined as point of the zero large-signal polarization P.

To explain this, the intrinsic contribution has to be investigated as well. No matter if a unit cell is switched upwards or downwards, its intrinsic, e.g., lattice shift, contribution to the polarization is in the field direction. Therefore, to measure a zero large-signal polarization, slightly more cells must be switched downwards than upwards in order to compensate for the intrinsic polarization contribution (arrow in

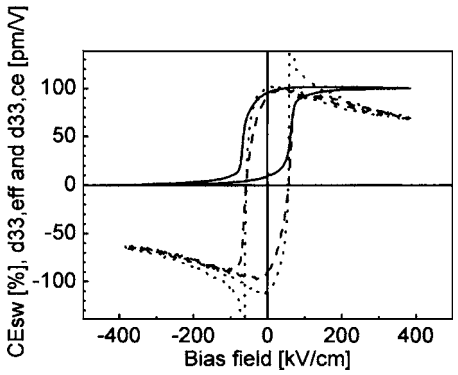

FIG. 4. Calculated percentage of unit cells switched ce_{sw} (line), measured effective electromechanical small-signal response $d_{33,eff}$ (dashes, $f_{bias}=1$ Hz, $f_{ac}=8$ kHz, and $V_{ac}=100$ mV), and calculated electromechanical small-signal response per unit cell $d_{33,c}$ (dots) of 130 nm PZT (45/55).

inset). Hence, there is a difference between the coercive fields measured in the large-signal polarization P and its irreversible contribution P_{irr}.

Another noteworthy fact is that both curves P and P_{rev} were symmetrized along the P axis. Therefore, asymmetries cannot be seen in either P_{irr} or ce_{sw}. Hence, unit cells contributing to the intrinsic behavior of the sample but not to the extrinsic switching processes are not accounted for during the calculation. This has to be considered in the further use of ce_{sw}.

To gain ce_{sw}, the irreversible contribution to the polarization has to be normalized and shifted by the following equation:

$$ce_{sw}=\left(\frac{P_{irr}}{P_{irr,max}-P_{irr,min}}+0,5\right)100, \tag{3}$$

where $P_{irr,max}$ and $P_{irr,min}$ are the maximal and minimal values of the irreversible contribution, respectively. Besides the result of this calculation, the effective field-induced electromechanical small-signal coefficient $d_{33,eff}$ is shown in Fig. 4. As seen in prior measurements,[11,13] the $d_{33,eff}$ curve is closed in the positive and negative saturations. On the other hand, the ce_{sw} curve indicates an ongoing change of the switching state of the sample. This can also be seen in the electric large-signal polarization (Fig. 3) and the measured field-induced electromechanical large-signal strain S, which is depicted in Fig. 5.

IV. MODELING OF THE LARGE-SIGNAL STRAIN

Also shown in Fig. 5 are the integrated $d_{33,eff}$ curve and the sample strain calculated by the model introduced by Bolten *et al.*[12] The former clearly shows why the simple integration of the electromechanical small-signal response by

$$S=\int d_{33,eff}dE \tag{4}$$

is insufficient to model the large-signal strain S. Since the integration circles around the enclosed area in the $d_{33,eff}$ curve, the resulting end point of the integration deviates from zero by a value ΔS. This behavior is due to the missing

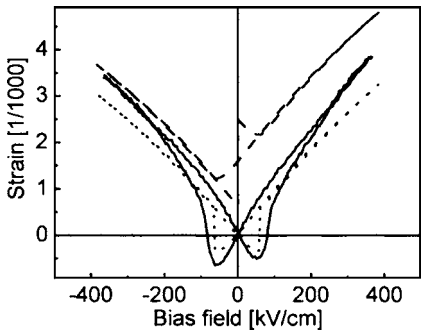

FIG. 5. Measured electromechanical large-signal strain S (line, $f_{bias}=123$ Hz), integrated electromechanical small-signal response (dashes), and calculated electromechanical large-signal response (the model of Bolten *et al.*, dots) of 130 nm PZT (45/55).

incorporation of the indirect extrinsic influences on the intrinsic response.[11]

The simplest solution is to assume two abrupt switching processes at the respective coercive voltages and add $\Delta S/2$ at these points. As shown above, this model has several drawbacks.

A first improvement of the model is to incorporate a linear approximation of the switching behavior near the coercive voltage. Investigation of either the polarization, the $d_{33,eff}$, or the ce_{sw} curve can be used to gain the field intervals inside which $\Delta S/2$ is then added continuously to the result of the integrated $d_{33,eff}$ curve. The result is shown in Fig. 6 (dots). Though this improvement can model backswitching of the sample to a certain degree, it is still insufficient to explain any switching effects during saturation of the sample. Hence, the calculated strain curve is still closed in these regimes.

The next step is to fully use the knowledge about the switching state ce_{sw} of the sample and expand Eq. (4) to

$$S=\int d_{33,eff}dE+\frac{\Delta S}{2}ce_{sw} \tag{5}$$

for calculations coming from negative saturation and going to positive saturation and

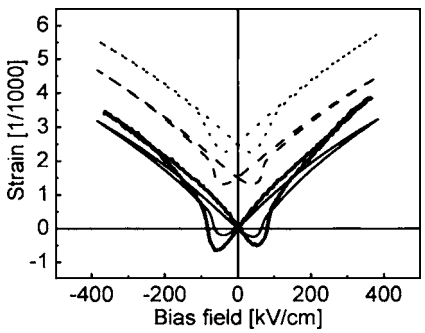

FIG. 6. Measured electromechanical large-signal strain S (bold line, $f_{bias}=123$ Hz) and calculated electromechanical large-signal response (miscellaneous models, line, dashes, and dots shifted along the strain axis for improved readability) of 130 nm PZT (45/55).

$$S = \int d_{33,\mathrm{eff}} dE + \frac{\Delta S}{2}(1 - \mathrm{ce}_{\mathrm{sw}}) \tag{6}$$

for the calculation of the other direction of bias changes. As can be seen from Fig. 6 (dashes), this calculation is able to model the switching influence near the coercive voltage and in saturation.

However, the used equations have a drawback: They assume that each switching process has the same impact on the sample strain S. As was indicated in Ref. 11, the intrinsic strain change of a switching unit cell $\Delta l_{\mathrm{switch}}$ is dependent on the strain Δl of the unit cell before the switching process. Hence, the influence of a single extrinsic switching process on the intrinsic sample strain should increase for higher sample strains S at the time of the switching.

In order to improve the equations, the intrinsic strain of the sample has to be investigated in more detail. One approach is to think of the strain of the sample as the sum of the strains of all unit cells. Also, unit cells switched in opposite directions strain against each other and therefore decrease the large-signal strain S of the sample. Hence, the large-signal strain of the sample can be calculated by

$$S = \int d_{33,\mathrm{ce,up}} \mathrm{ce}_{\mathrm{sw}} + d_{33,\mathrm{ce,dw}}(1 - \mathrm{ce}_{\mathrm{sw}}) dE, \tag{7}$$

where $d_{33,\mathrm{ce,up}}$ and $d_{33,\mathrm{ce,dw}}$ are the effective electromechanical small-signal coefficients of the unit cells switched upwards and downwards, respectively. Since these values are unknown, the approximation

$$d_{33,\mathrm{ce,up}} = -d_{33,\mathrm{ce,dw}} = d_{33,\mathrm{ce}} \tag{8}$$

is used. However, as can be seen in Fig. 4, where $d_{33,\mathrm{ce}}$ was calculated by

$$d_{33,\mathrm{eff}} = d_{33,\mathrm{ce}} \mathrm{ce}_{\mathrm{sw}} - d_{33,\mathrm{ce}}(1 - \mathrm{ce}_{\mathrm{sw}}) = d_{33,\mathrm{ce}}(2\mathrm{ce}_{\mathrm{sw}} - 1) \Rightarrow d_{33,\mathrm{ce}} = \frac{d_{33,\mathrm{eff}}}{(2\mathrm{ce}_{\mathrm{sw}} - 1)}, \tag{9}$$

the values are decreasing monotonously for increasing positive bias fields above the coercive field. Therefore, the absolute value should be increased for unit cells oriented against the direction of the applied electric field. Hence, the errors are introduced to the model by this approximation. Additionally, the combination of Eqs. (7) and (9) leads only back to Eq. (4), since any extrinsic influences are lost.

However, Eq. (7) can also be written as

$$S = S_{\mathrm{ce,up}} \mathrm{ce}_{\mathrm{sw}} + S_{\mathrm{ce,dw}}(1 - \mathrm{ce}_{\mathrm{sw}}), \tag{10}$$

where $S_{\mathrm{ce,up}}$ and $S_{\mathrm{ce,dw}}$ are the electromechanical large-signal strains of the unit cells switched upwards and downwards, respectively, or, using the approximation

$$S = S_{\mathrm{ce}}(2\mathrm{ce}_{\mathrm{sw}} - 1). \tag{11}$$

Here, the large-signal sample strain is proportional to $(2\mathrm{ce}_{\mathrm{sw}} - 1)$. This can be used to incorporate changes of the sample switching state in a stepwise calculation of the large-signal sample strain:

$$S_{i+1} = [S_i + d_{33,r,i+1}(E_{i+1} - E_i)] \frac{(2\mathrm{ce}_{\mathrm{sw},i+1} - 1)}{(2\mathrm{ce}_{\mathrm{sw},i} - 1)}. \tag{12}$$

While the first part is the simple numerical integration equivalent to Eq. (4), the second part accounts for changes of the sample switching state. The result of this calculation is also shown in Fig. 6 (line).

V. DISCUSSION

This model, despite the approximation used, is able to reflect switching influences on the large-signal strain S near the coercive field and in saturation. The shape of the resulting curve is comparable to the measured large-signal strain. However, several differences are notable. First, the coercive field is decreased in the calculated curve, which can be attributed to the difference of the measurement frequency.[12] Second, the maximum value of calculated strain is decreased in comparison to the measured value. This can result from the approximation [Eq. (8)] used as well as influences of the measurement parameters or direct extrinsic effects. The clarification of the cause for the latter difference will be investigated in the future.

Another interesting fact to note is that the final model does not need any precalculation of the small-signal coefficient $d_{33,\mathrm{eff}}$ to gain ΔS. Instead, it is sufficient to shift the curve for the switching state of the unit cells $\mathrm{ce}_{\mathrm{sw}}$ along the $\mathrm{ce}_{\mathrm{sw}}$ axis in order to account for unit cells clamped into one direction. This is done until the resulting strain curve has the same start and end points of zero strain at a bias field of zero. Thus, it is found that approximately 8% of the active unit cells are clamped into the negative Z direction. Hence, the model is also the one able to account for asymmetries in the switching behavior.

The errors introduced by the approximation should be negligible in saturation, since most of the unit cells are switched into the same direction. Hence, the model should be accurate in this regime and shows clearly that the curve is open though the measured curve for the electromechanical small-signal coefficient $d_{33,\mathrm{eff}}$ is closed in saturation. This indicates that the electromechanical small-signal behavior of the sample can be the same for different strains and/or switching configurations. A first explanation for this fact can be found by investigating an increase in the percentage of unit cells switched in the positive Z direction under an application of a constant bias field. If the field is also applied in

the positive Z direction, the sample strain would increase due to lesser cells trying to contract the sample. Hence, the intrinsic strain of each unit cell is increased as well. Combining this with the decreasing electromechanical small-signal behavior for increasing fields and/or strains, this would lead to a decrease of the coefficient $d_{33,ce}$ of the unit cells. Thus, the resulting electromechanical small-signal coefficient $d_{33,eff}$ of the sample is either increased, equaled, or decreased in comparison to the value before the switching process. One method of finding further proof for this model could be the numerical simulation of a system containing multiple unit cells. This simulation could also lead to further insights providing a method to gain the values of $d_{33,ce,up}$ and $d_{33,ce,dw}$ from the measurements and improving the presented model even further.

VI. CONCLUSIONS

The influences of reversible and irreversible switching processes on the electromechanical large-signal strain S were discussed in detail. By calculating the percentage of switched unit cell ce_{sw}, it was possible to improve the older model for the calculation of the field-induced electromechanical large-signal strain S. Differences between the calculated and measured large-signal strains were discussed and explained. In particular, the behavior in sample saturation was investigated. Finally a model was presented elucidating this behavior.

[1]N. Setter, *Piezoelectric Materials in Devices* (Ceramics Laboratory, EPFL Swiss Federal Institute of Technology, Switzerland, 2002).
[2]H. Schaumburg, *Keramik* (Teubner, Stuttgart, 1994).
[3]KFA Juelich, 26 IFF-Ferienkurs (1995).
[4]Q. M. Zhang, W. Y. Pan, S. J. Jang, and L. E. Cross, J. Appl. Phys. **64**, 6445 (1988).
[5]W. Pan, S. Sun, and P. Fuierer, J. Appl. Phys. **74**, 1256 (1993).
[6]Q. M. Zhang, H. Wang, N. Kim, and L. E. Cross, J. Appl. Phys. **75**, 454 (1994).
[7]N. A. Pertsev and A. Yu. Emelyanov, Appl. Phys. Lett. **71**, 3646 (1997).
[8]D. V. Taylor and D. Damjanovic, Appl. Phys. Lett. **76**, 1615 (2000).
[9]S. Y. Chen and C. L. Sun, J. Appl. Phys. **90**, 2970 (2001).
[10]D. Bolten, U. Böttger, and R. Waser, J. Appl. Phys. **93**, 1735 (2003).
[11]P. Gerber, C. Kügeler, U. Böttger, and R. Waser, J. Appl. Phys. **95**, 4976 (2004).
[12]D. Bolten, U. Böttger, and R. Waser, J. Eur. Ceram. Soc. **24**, 725 (2004).
[13]P. Gerber, K. Prume, A. Roelofs, C. Kügeler, U. Böttger, and R. Waser, J. Appl. Phys. **96**, 2800 (2004).
[14]P. Gerber, A. Roelofs, O. Lohse, C. Kügeler, S. Tiedke, U. Böttger, and R. Waser, Rev. Sci. Instrum. **74**, 2613 (2003).
[15]B. Noheda, D. E. Cox, G. Shirane, J. A. Gonzalo, L. E. Cross, and S. -E. Park, Appl. Phys. Lett. **74**, 2059 (1999).
[16]C. Kügeler, M. Hoffmann, U. Böttger, and R. Waser, Proc. SPIE **4699**, 114 (2002).